GEOPHYSICAL RESEARCH LETTERS, VOL. 25, NO.12, PAGES 2033-2036, JUNE 15, 1998

The auroral current circuit and field-aligned currents observed by FAST

R. C. Elphic[1], J. W. Bonnell[1], R. J. Strangeway[2], L. Kepko[2], R. E. Ergun[3], J. P. McFadden[3], C. W. Carlson[3], W. Peria[3], C. A. Cattell[4], D. Klumpar[5], E. Shelley[5], W. Peterson[5], E. Moebius[6], L. Kistler[6], R. Pfaff[7]

Abstract. FAST observes signatures of small-scale downward-going current at the edges of the inverted-V regions where the primary (auroral) electrons are found. In the winter pre-midnight auroral zone these downward currents are carried by upward flowing low- and medium-energy (up to several keV) electron beams. FAST instrumentation shows agreement between the current densities inferred from both the electron distributions and gradients in the magnetic field. FAST data taken near apogee (~4000-km altitude) commonly show downward current magnetic field deflections consistent with the observed upward flux of ~10^9 electrons cm^{-2} s^{-1}, or current densities of several μA m^{-2}. The electron, field-aligned current and electric field signatures indicate the downward currents may be associated with "black aurora" and auroral ionospheric cavities. The field-aligned voltage-current relationship in the downward current region is nonlinear.

Introduction

One important issue in auroral physics specifically and magnetosphere/ionosphere coupling in general is how and where field-aligned currents close through the ionosphere and in the magnetosphere. FAST is uniquely suited to studying auroral microprocesses, but the particles and fields instruments also address questions of a more global nature, like the closure of field-aligned currents (FACs). FACs have been studied using rockets and satellites for decades - the new observations which FAST offers are high sensitivity, high time resolution plasma measurements with continuous monitoring of all pitch angles, and high time resolution measurements of fields. The signatures of auroral field-aligned currents are observed largely as east-west deflections in the background field, and are closely associated with north-south variations in the electric field at ionospheric altitudes [*Sugiura et al.*, 1982; *Sugiura,* 1984]. This relationship is observed to hold between magnetic field measurements at high altitudes and electric fields at low altitudes [*Weimer et al.*, 1985]. At the largest scales, magnetosphere-ionosphere coupling takes place in a voltage generator fashion, while at smaller scales it tends toward a current generator [*Lysak,* 1985; *Vickrey et al.*, 1986; *Weimer et al.*, 1987]. A relationship between upward field-aligned current density and parallel potential drop is sometimes observed [*Lyons et al., 1979; Weimer et al.*, 1987].

During the northern winter auroral campaign of 1997, the FAST fluxgate magnetometer observed small-scale regions of downward-going current, often associated with upgoing accelerated low- and medium-energy (up to about several keV) electron beams. The scale size of the downward currents can range from less than a kilometer (at FAST altitudes) up to tens of kilometers, usually concentrated at the edges of inverted-V structures. These upgoing electrons have occasionally been observed before [*Boehm et al.*, 1995; *Clemmons et al.*, 1995], but unlike previous missions, FAST offers continuous high-time-resolution systematic monitoring of particle distribution functions. Downward currents have previously been associated with diverging electric fields at satellite altitudes, and presumably with the "black aurora", the optical counterpart of bright discrete arcs [*Marklund et al.*, 1994; *Marklund,* 1997; *Marklund et al.*, 1997]. FAST data taken near apogee and near magnetic midnight commonly show downward FACs with current densities of between 2 and 4 μA m^{-2}, consistent with the observed upward electron flux of ~10^9 cm^{-2} s^{-1}. The downward current densities are greatest at locations mapping to minima in the inferred height-integrated Pedersen conductivity, and presumably are related to formation of ionospheric cavities, as observed by radar [*Williams et al.*, 1990; *Opgenoorth et al.*, 1990; *Aikio et al.*, 1993]. These fluxes are considerably larger than those discussed by *Doe et al.* [1995], in simulating the field-aligned current generation of auroral ionospheric cavities (AICs) in the F-region.

Here we focus on where the downward currents/upgoing electrons are found, namely the edges of inverted-V regions, and show how they appear to be smaller scale but more intense currents than those in the auroral precipitation regions. We explore ramifications for auroral circuit closure, and the voltage-current relationship for both upward and downward FACs.

Observations

The data come from a FAST pass through the winter auroral zone over Alaska, orbit 1773 on February 1, 1997 between about 21 and 22 MLT. The FAST trajectory for this occasion went from low to high northern latitudes. The geomagnetic conditions for the pass were very quiet, Kp 1^-, so the observed auroral zone was poleward of its average position. Figure 1 shows DC magnetic field, electron plasma analyzer data, and other derived quantities for this pass. The field data have been

[1]Los Alamos National Laboratory, Los Alamos, NM
[2]Institute of Geophysics and Planetary Physics, University of California, Los Angeles, CA
[3]Space Sciences Laboratory, University of California, Berkeley, CA
[4]University of Minnesota, Minneapolis, MN
[5]Lockheed Martin Palo Alto Research Laboratory, Palo Alto, CA
[6]University of New Hampshire, Durham, NH
[7]NASA/Goddard Space Flight Center, Greenbelt, MD

Paper number 98GL01158.
0094-8534/98/98GL-01158$05.00

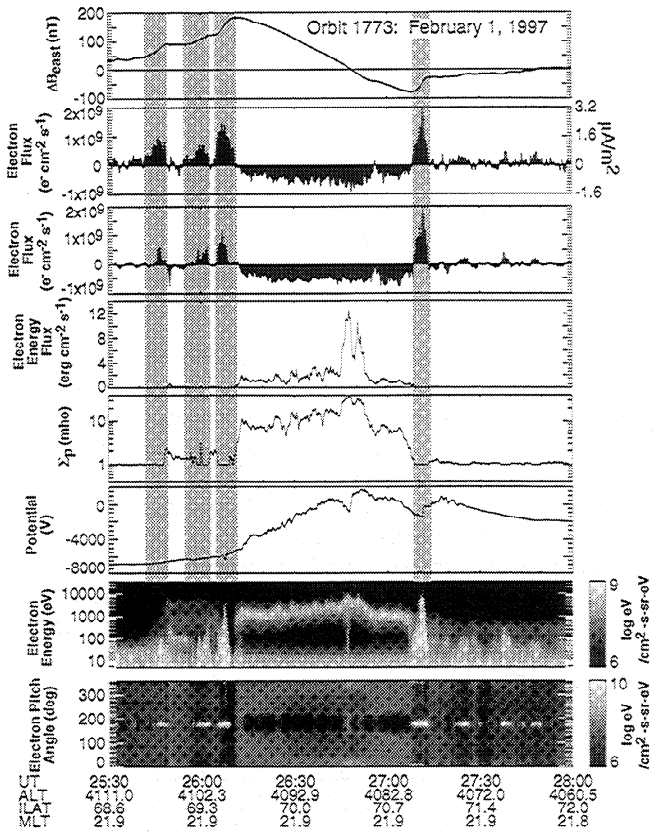

Fig.1. FAST data from a northern winter pre-midnight auroral zone pass on February 1, 1997. The magnetometer data have been detrended with IGRF 1995, with ΔB_{EAST} the magnetic deflection, positive east. The second and third panels show the estimated electron flux derived from a time-derivative of the magnetic field variation, and the measured flux, respectively. The fourth and fifth panels show the precipitating electron energy flux mapped to 100-km altitude, and the resulting height-integrated Pedersen conductivity. The sixth panel shows the electrostatic potential obtained by integrating the measured electric fields along the flight path of the satellite. The bottom two panels show the electron energy spectrum (summed over all pitch angles) and the electron pitch angle spectrum (summed over all energies). Grey vertical bars denote regions of downward current.

detrended using the model field, IGRF 1995; the top panel corresponds to the east-west excursions. The plots go from lower to higher latitudes, starting at about 69° and ending at about 74° ILAT. A positive slope of ΔB_{EAST} corresponds to a downward current, a negative slope to an upward current.

The bottom two panels show the electron energy spectrum between 5 eV and about 30 keV, summed over all pitch angles, and the electron pitch angle spectrum summed over all energies. Angles of 0° and 360° correspond to field-aligned, or downgoing electrons, while 180° is upgoing from the ionosphere. The atmospheric loss cone shows up clearly between roughly 150° and 210° from 0926 to 0927:10 UT.

At lower latitudes, roughly isotropic plasma sheet electrons are observed, which at higher, sub-auroral latitudes are interspersed with upgoing accelerated electron beams. This region corresponds to the downward FAC signature in the magnetic field. Then FAST passes into the auroral acceleration region proper, with inverted-V electron structure, lasting roughly a minute during which the spacecraft moves about 360 km. The field variation in this region is entirely due to upward FAC, as one would expect. This is followed by a brief but very intense upgoing electron beam, with energies going up to nearly 10 keV. The cumulative downward current carried by all these upgoing electron beams roughly balances the total upward current in the inverted-V region, and by the time FAST has gone up to 74° the perturbation field has returned to nearly its starting point, indicating that little net current was flowing into or out of the auroral ionosphere locally in this case.

Panel 2 shows the inferred "electron flux" obtained by taking the time derivative of the field variations and ascribing them to spacecraft motion through stationary field-aligned current sheets; flux = $(1/\mu_0 e)\cdot(1/v_{S/C})\cdot\partial B_{EAST}/\partial t$. Panel 3 shows the calculated total electron flux from the electron plasma analyzers (integrated from 50 eV up to 30 keV). The two plots are on the same scale and show good agreement for both upgoing electron beams and downgoing, inverted-V electrons. Thus the upgoing accelerated electrons represent the bulk of the current carriers in the downward FACs, just as downgoing accelerated electrons are the principal charge carriers in the primary auroral acceleration region. The upgoing electron currents are spatially limited in extent, while the currents in the inverted-V region are broader and less intense in the case shown here.

Panels 4 and 5 add two more quantities to the picture, namely the precipitating electron energy flux mapped to 100-km altitude (the net electron energy flux which makes it to 100 km in the ionosphere), and an estimate of the height-integrated Pedersen conductivity based on the precipitating electron energy flux and characteristic energy. To place this pass in the context of observable optical aurora, the threshold for 1 kR of 5577 Å emissions at 100 km is roughly 0.6 to 0.8 ergs cm^{-2} s^{-1} [*Steele and McEwen,* 1990]. The height-integrated Pedersen conductivity is based on a formulation by *Robinson et al,* [1987], $\Sigma_P = 40\ E_C\ \Phi_E^{1/2}/(16 + E_C^2)$, where Σ_P is the height-integrated conductivity in mhos, E_C is the electron characteristic energy in keV and Φ_E is the precipitating electron energy flux in ergs cm^{-2} s^{-1}. We assume the background ionospheric conductivity never drops below 1 mho, but it may well be less than 1 mho due to E- and F-region cavity formation in the downward current regions. The upward electrons/downward currents are found where there is little or no electron energy flux deposition to the ionosphere. The sites of greatest electron energy deposition are not well correlated with larger upward field-aligned current in this case.

The sixth panel shows the potential obtained by integrating the (approximately) north-south component of the DC electric field, which effectively filters out the small-scale electrostatic shock electric fields. There is an overall trend in the potential which presumably relates to the large scale convection in the magnetosphere and ionosphere. At lower latitudes, between 0925:30 and 0926:50 UT, the electric potential increases generally monotonically, consistent with a northward electric field and sunward convection in the ionosphere. After this time the potential decreases, on average, and is consistent with antisunward convection. Intermediate-scale structure in the potential within and at the edges of the inverted-V region probably does not map to the ionosphere: reversals in the ionospheric E field should be reflected in reversals of ΔB_{EAST}.

To summarize, the observed downward currents are found at the edges of the inverted-V region, and occur in narrow regions of relatively high current density. For these cases, the north-south scale size of the downward current regions is about 30 km at FAST, or roughly 10 km at 100-km altitude. By con-

trast, the upward FAC/inverted-V region extends over hundreds of kilometers, with a lower average current density. This pass is representative of many FAST quiet-time, pre-midnight passes during the winter campaign.

Discussion

For static conditions, the field-aligned current density, $j_{||}$, is required by continuity to close through the ionosphere, and relates to the ionospheric horizontal conductivity and electric field by $j_{||} = -\nabla\cdot\boldsymbol{J}_\perp = -\nabla\cdot(\boldsymbol{\Sigma}\cdot\boldsymbol{E})$ where $\boldsymbol{J}_\perp$ is the height-integrated horizontal current density and $\boldsymbol{\Sigma}$ is the height-integrated Pedersen conductivity. Then, except for a mapping factor from FAST to the ionosphere, $\Delta B_{EAST} = \boldsymbol{J}_\perp/\mu_o = \Sigma_P \boldsymbol{E}/\mu_o$. In the voltage generator scenario, the magnetosphere sets the spatial potentials and hence the electric fields: For a constant $\boldsymbol{E}$, field aligned currents result from gradients in the conductivity. For example, at the edge of the inverted-V region there is a conductivity gradient, and in the absence of a compensating electric field gradient this would force a closure current of upgoing electrons at the edge of the inverted-V region. But one observes that the downward FACs occur not at the principal conductivity gradients but rather outside them, in what we assume to be AICs. In the current generator scenario, the ionospheric electric fields adjust to provide the current flow required by the magnetosphere. Since ΔB_{EAST} varies smoothly while the inferred Σ_P varies considerably throughout the auroral region, it appears that the winter premidnight ionospheric electric field is structured to provide a smoothly varying current distribution. This suggests the current generator picture is possibly the more correct for the passes shown here.

Part of the auroral circuit involves potential drops along field lines, where the FACs flow. Figure 2 shows the relationship between the log of the magnitude of the inferred field-aligned potential drop and the field-aligned current density observed between 0925:40 and 0929:30 UT during the orbit 1773

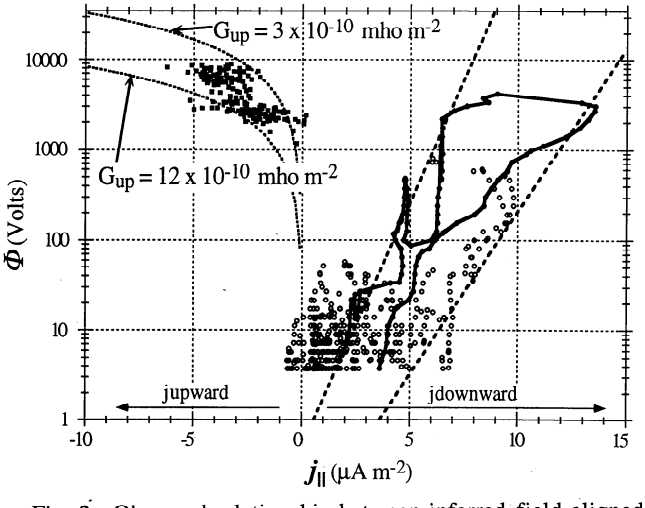

Fig. 2. Observed relationship between inferred field-aligned potential drop and field-aligned current density for the auroral pass shown in Figure 1. Upward current due to precipitating auroral electrons is anti-parallel to the ambient magnetic field (hence negative, left), while downward currents are parallel to the ambient fields (hence positive, right). These data clearly demonstrate the well-known voltage-current relationship for inverted-V current systems, while a non-linear relationship holds for downward currents.

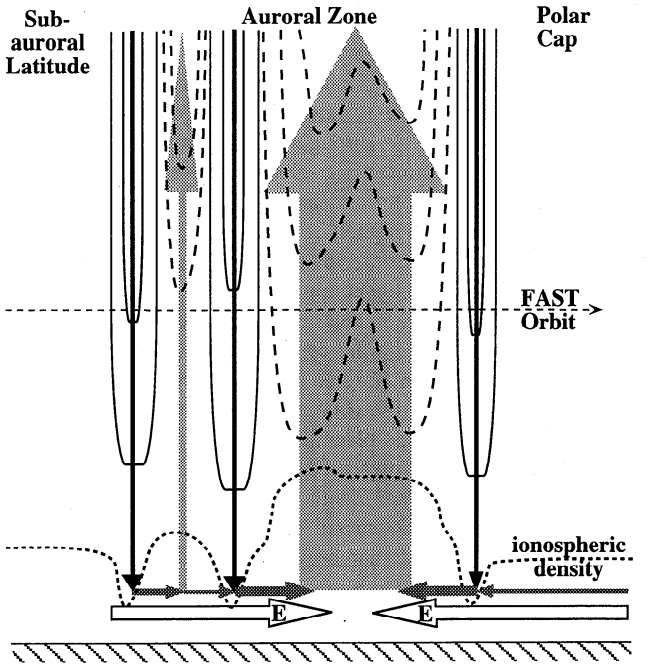

Fig. 3. Schematic of the auroral zone, showing current closure in the presence of ionospheric electric fields and high-altitude potential structure associated with both inverted-V and upward accelerated electrons (dashed contours denote negative potentials). The dotted line denotes column-integrated ionospheric density.

auroral pass of Figure 1. This interval includes the inverted-V region and the downward current sheets found outside it. Both downward (positive) and upward (negative) current densities have been mapped to 100-km altitude. The field-aligned potential drop for the upward current region is assumed to be given by the sum of the precipitating auroral electron beam energy and the energy of the upgoing ion beam (if any, for cases where the potential structure extends below the satellite). For the downward current sheet, we use the upper energy cutoff of the upgoing accelerated electrons as an estimate of the field-aligned potential drop below the spacecraft.

It can be seen that the relationship between parallel potential drops and field-aligned current is different for downward and upward currents. For upward currents, we show the results for a field-aligned conductivity (the Lyons-Evans-Lundin constant) G_{up} of $j_{||}/V_{||}$ = 3 x 10^{-10} and 1.2 x 10^{-9} mho m^{-2} (other workers have found values ranging between 10^{-10} and 10^{-8} mho m^{-2}). For downward currents, the relationship is clearly nonlinear - as current density increases, the potential drop grows exponentially. The data for the downward current sheet at 0927:15 UT is plotted as a solid line, as an example. Inspecting Figure 2, we pose a form $\Phi = \Phi_o\cdot\exp(j/j_o)$, and define an effective conductivity $G_{down} = (\partial\Phi/\partial j)^{-1} = j_o/\Phi_o\cdot\exp(-j/j_o)$. This form implies that the field-aligned conductivity diminishes exponentially with increasing downward current density. The two dashed lines in Figure 2 correspond to j_o/Φ_o of 1.6 x 10^{-6} and 2 x 10^{-5} mho m^{-2}. Our interpretation of this result is that it is initially easy to draw dense current from the ionosphere, since $j_o/\Phi_o >> G_{up}$, but it rapidly becomes more difficult to do so, possibly due to evacuation of charge carriers, and possibly due to wave turbulence. The data suggest that the relationship changes even within a single downward current region, and we suspect that this has to

do with spatial and temporal variations in ionospheric density brought on by cavity formation.

In Figure 3 we show the FAST auroral zone and the winter pre-midnight ionosphere it connects to. Solid arrows show the sense of current flow through the auroral ionosphere and along field lines. Ionospheric electric fields are denoted by open arrows. At the bottom of the inverted-V region the ionospheric density is higher than in surrounding regions because the precipitating electrons enhance the ambient ionization. Because ionospheric convection is out of the page in the north, and into the page in the south, the ionospheric electric fields point inward toward the center of the inverted-V region. At around 100 km, the horizontal current is carried by ions moving along E, and the $\boldsymbol{JxB}$ force is such as to maintain transport in the presence of collisional friction. This diagram has elements of those presented by *Blixt and Brekke* [1996] and *Marklund et al.* [1997], with the addition of parallel potential structures in the downward current regions. The auroral circuit consists of loads not only in the ionosphere, but also where FACs flow in the auroral acceleration regions. For orbit 1773 there is a several kV potential drop between the magnetosphere and the ionosphere below the inverted-V region, another approximately 10 kV drop within the ionosphere, and another several kV drop between the subauroral ionosphere and the magnetosphere.

We are still left with the question of why the downward current tends to occur in several distinct smaller-scale intense FACs, while the upward currents are broader, less structured and less intense. The downward current excavates an AIC in tens to hundreds of seconds [*Doe et al,* 1995]. In simulations of cavity formation, it was found that currents appear to reach a limiting value, beyond which the plasma loss rate does not increase. Together with a possible upper limit on current density (or on field-aligned conductance), the downward FAC scale size places a limit on how much total current can be returned in any one region. So if a given downward FAC/AIC is not sufficient to return all the ionospheric current, the current may be forced to close at another site. One way of looking at this is that a given current channel may become more resistive, and force the development of another channel. This is a modification of the magnetospheric current generator picture - the ionosphere feeds back on the generator and chooses where the currents will close.

Another reason for the structuring of the downward FACs may relate to the magnetospheric boundary conditions. Since $\Delta B_{EAST} \sim J_{\perp}/\mu_o$, it can be regarded as a rough proxy for the ionospheric $\boldsymbol{JxB}$ force. This quantity relates to how hard the magnetosphere is "tugging" on the ionosphere, and may reflect the presence of a kind of turbulence in or layering of convection in the plasma sheet [*Borovsky et al.*, 1997]. However, we would expect similar structure in the inverted-V region as well, which is not seen in the case shown here.

Acknowledgments. This work was supported by NASA order number S-57795-F. We are grateful to the entire FAST team for comments and suggestions, to Joe Borovsky for discussions, and to the two referees for helpful, constructive criticism.

References

Aikio, A. T., et al., Ground-based measurements of an arc-associated electric field, *J. Atmos. Terr. Phys., 55,* 797-808, 1993.

Blixt, E. M., and A. Brekke, A model of currents and electric fields in a discrete auroral arc, *Geophys. Res. Lett., 23,* 2553-2556, 1996.

Boehm, M. H., et al. Observations of an upward-directed electron beam with the perpendicular temperature of the cold ionosphere, *Geophys. Res. Lett., 22,* 2103,1995.

Borovsky, J. E., et al., The Earth's plasma sheet as a laboratory for flow turbulence in high-β MHD, *J. Plasma Physics, 57,* 1-34, 1997.

Clemmons, J. H., et al., Upwardly accelerated auroral electrons: The role of parallel electric fields (abstract), *EOS Trans. Am. Geophys. Union, 76,* F551, 1995.

Doe, R. A., et al., Electrodynamic model for the formation of auroral ionospheric cavities, *J. Geophys. Res., 100,* 9683, 1995.

Lyons, L. R., et al., Observed relation between magnetic-field aligned electric fields and downward electron-energy fluxes in the vicinity of auroral forms, *J. Geophys. Res., 84,* 457-461, 1979.

Lysak, R. L., Auroral electrodynamics with current and voltage generators, *J. Geophys. Res., 90,* 4178, 1985.

Marklund, G., Auroral phenomena related to intense electric fields observed by the Freja satellite, *Plasma Phys. Control. Fusion, 39,* 195, 1997.

Marklund, G., T. Karlsson, and J. Clemmons, On low-altitude particle acceleration and intense electric fields andtheir relationship to black aurora, *J. Geophys. Res., 102,* 17,509, 1997.

Marklund, G., et al., On intense diverging electric fields associated with black aurora, *Geophys. Res. Lett., 21,* 1859, 1994.

Opgenoorth, H. J., et al., Regions of strongly enhanced perpendicular electric-fields adjacent to auroral arcs, *J. Atmos. Terr. Phys., 52,* 449-458, 1990

Robinson, R. M., et al., On calculating ionospheric conductances from the flux and energy of precipitating electrons, *J. Geophys. Res., 92,* 2565, 1987.

Steele, D. F., and D. J. McEwen, Electron auroral excitation efficiencies and intensity ratios, *J. Geophys. Res., 95,* 10,321, 1990.

Sugiura, M., et al., Initial results on the correlation between the magnetic and electric fields observed from the DE-2 satellite in the field-aligned current regions, *Geophys. Res. Lett., 9,* 985, 1982.

Sugiura, M., A fundamental magnetosphere-ionosphere coupling mode involving field-aligned currents as deduced from DE-2 observations, *Geophys. Res. Lett., 11,* 877-880, 1984.

Vickrey, J. F., et al., On the current-voltage relationship of the magnetospheric generator at intermediate spatial scales, *Geophys. Res. Lett., 13,* 495-498, 1986.

Weimer, D., et al.., Auroral zone electric fields from DE 1 and DE 2 at magnetic conjunctions, *J. Geophys. Res., 90,* 7479, 1985.

Weimer, D. R., et al., The current-voltage relationship in auroral current sheets, *J. Geophys. Res., 92,* 187-194, 1987.

Williams, P. J. S., et al., High-resolution measurements of magnetospheric electric fields, *J. Atmos. Terr. Phys., 52,* 439-448, 1990.

J. Bonnell, R. Elphic, Space and Atmospheric Sciences Group, MS D466, Los Alamos National Laboratory, Los Alamos, NM 87545 (e-mail: relphic@lanl.gov)

L. Kepko, R. Strangeway, Institute of Geophysics and Planetary Physics/UCLA, Los Angeles, CA 90095

C. Carlson, R. Ergun, J. McFadden, W. Peria, Space Sciences Laboratory, University of California, Berkeley. CA 94720

C. Catttell, University of Minnesota, Minneapolis, MN 55455

D. Klumpar, W. Peterson, E. Shelley, Lockheed Martin Palo Alto Research Laboratory, Palo Alto, CA 94304

L. Kistler, E. Moebius, University of New Hampshire, Durham, NH 03824

R. Pfaff, Code 696, NASA/Goddard Space Flight Center, Greenbelt, MD 20771

(Received December 1, 1997; revised March 17, 1998; accepted March 25, 1998)